Fabrication and Characterization of Polymer Membrane from PET Waste Using Chitosan Synthesized from Snail Shell

Matthew Chukwu[1], Ikiode Confidence[2], James Isaiah[3], Ewere Donatus[4]

[1,2,3]*Department of Polymer Technology, Auchi Polytechnic, Auchi, Edo State, Nigeria*
[1,2,3]*Auchi Polytechnic Centre of Excellence in Creative Innovation and Entrepreneurship Dynamics, Auchi, Edo State, Nigeria.*
[4]*Department of Chemical and Petroleum Engineering, Afe Babalola University, Ado-Ekiti, Ekiti State, Nigeria*

Abstract— Nigeria faces a significant plastic waste problem, with only 12% of the 2.5 million tons of plastic waste produced annually being recycled. This study focuses on the development and characterization of a polymer membrane fabricated from recycled Polyethylene Terephthalate (PET) bottles and chitosan derived from snail shells. PET bottles were collected, cleaned, and processed into fine particles, while snail shells were demineralized and deacetylated to produce chitosan. A dope solution was prepared by dissolving PET in trifluoroacetic acid and incorporating chitosan, which was then cast into a membrane using the solution casting method. The resulting membrane was characterized using Fourier transform infrared (FTIR) spectroscopy, scanning electron microscopy/energy dispersive X-ray spectroscopy (SEM/EDX), and thermogravimetric analysis/differential thermal analysis (TGA/DTA). FTIR analysis confirmed the presence of functional groups associated with PET and chitosan, indicating successful incorporation of both components into the membrane. SEM/EDX analysis revealed a compact and consistent surface morphology with no visible large pores, and the presence of carbon, oxygen, calcium, and nitrogen, suggesting the integration of chitosan and residual mineral phases from the snail shells. TGA/DTA analysis demonstrated the thermal stability of the membrane up to 300 °C, with a multi-phase degradation pattern influenced by the presence of PET, chitosan, and inorganic residues. The increased char formation due to chitosan and inorganic substances suggests potential flame-retardant properties. This study demonstrates the feasibility of transforming PET waste and chitosan derived from snail shells into functional composite membranes, offering a sustainable approach to plastic waste management and resource utilization.

Keywords: *Recycled PET bottles, Chitosan, Polymer membrane, Plastic waste, Fourier transform infrared, Scanning electron microscopy, Thermogravimetric analysis*.

I. Introduction

In Nigeria, around 2.5 million tons of plastic waste is produced each year, with only about 12% being recycled. This leaves a significant amount of waste in landfills, waterways, rivers, and oceans, posing an environmental hazard (Aare et al., 2024). The primary reasons for the high consumption of single-use plastics, such as water sachets, PET bottles, food packaging, straws, and plastic toys, include inadequate waste management, insufficient recycling infrastructure, and a general lack of environmental awareness (Uchechukwu Nwafor, 2024) among the population (Solaja et al., 2024). Significant factors contributing to the high levels of plastic waste include the swift increase in population, inadequate waste management systems and attitudes, and the intentional neglect by the government and its agencies to raise public awareness about proper plastic waste disposal (Villanueva et al., 2021). Enhancing the management of plastic water, investing in recycling facilities, minimizing single-use plastics, and promoting research into the sustainable utilization of plastic waste as raw materials for sustainable development are essential. Some industries are beginning to use plastic waste to create new products in construction, textiles, and various engineering fields (Nuruzzaman et al., 2025; Oladele et al., 2024). Due to the rapid increase in population, many people around the world now rely on bottled water for drinking and household purposes because they lack access to high-quality portable water. These bottles, primarily composed of polyethylene terephthalate (PET), are often discarded after a single use and remain in the environment because they do not degrade (Villanueva et al., 2021)

The high levels of plastic waste are driven by several significant factors related to production, consumption, management, and socio-economic practices. One major factor is the rapid global increase in plastic production and consumption, especially single-use plastics, which are predominant contributors to environmental pollution. Urbanization and changes in living patterns have accelerated plastic consumption rates, leading to substantial plastic waste generation annually (Shin et al., 2020; Thanh et al., 2024). Insufficient waste management infrastructure and lack of technical capacity for hazardous waste management are critical contributors. Many regions, particularly in developing countries, face challenges due to inadequate recycling and resource recovery facilities. This leads to improper disposal, leakage of plastics into terrestrial and aquatic environments, and accumulation in water bodies where they persist for extended periods without effective clean-up (Kibria et al., 2023; Thanh et al., 2024). Low public awareness and inconsistent implementation of policies further exacerbate the plastic waste problem. In some Nigeria, lack of awareness of waste regulations results in insufficient adherence to waste

reduction and recycling measures at the household and community levels (). Moreover, disparities in policy enforcement among governments hinder uniform progress in waste mitigation (Chen et al., 2021; Kibria et al., 2023).

The global trade in plastic waste has also contributed to pollution problems, as importing countries may experience environmental degradation when handling imported plastic waste. For example, before China's 2018 ban on plastic waste imports, cities receiving such imports faced increased air pollution due to waste incineration processes. This highlights the transboundary nature of the plastic waste challenge and the environmental costs for recipient countries (Unfried & Wang, 2024). In addition to production and policy factors, the durability and chemical properties of plastics make them persistent in the environment, accumulating as debris in coastal lagoons, rivers, and oceans. Improper management of floating and settled plastic waste contributes significantly to contamination of aquatic ecosystems, affecting conservation areas and biodiversity. Seasonal changes and hydrological processes also influence the transport and accumulation patterns of plastic debris in such environments (Lorenzi et al., 2020; Thanh et al., 2024). Finally, the economic cost and challenges associated with recycling and effective processing of plastic waste limit the adoption of sustainable practices. Many recycling methods currently face drawbacks including high costs, reduced quality of recycled products, and technological limitations. The lack of economically viable and widely applied upcycling technologies restricts the potential to convert plastic waste into valuable materials and thus reduces incentive for waste diversion from disposal (Roy et al., 2021).

In summary, the significant factors contributing to high plastic waste levels include rapid production and consumption of predominantly single-use plastics, insufficient waste management infrastructure, low public awareness and enforcement of regulations, challenges due to global plastic waste trade, environmental persistence and improper disposal of plastics, and economic and technological barriers to effective recycling and upcycling (Chen et al., 2021; Kibria et al., 2023; Roy et al., 2021; Thanh et al., 2024; Unfried & Wang, 2024).

II. Materials and Methods

A. **Materials**

The research made use of discarded Polyethylene Terephthalate (PET) bottles, which were sourced from the Nestle Company located in Lagos, Nigeria. Chitosan, extracted from snail shells, was obtained from Auchi in Edo State, Nigeria. Additional materials included Cellulose Acetate from Loba-chemie in Mumbai, India, trifluoroacetic acid (TFA) also from Loba-chemie, Mumbai, India, Hydrochloric Acid with a purity of 97% from Loba Chemie, India, and Sodium Hydroxide (NaOH) with 97% purity from Molychem, Mumbai, India. These substances were diluted using deionized water to reach the required concentrations for the analytical procedures. All chemicals used were of analytical grade and were purchased commercially.

.B. **Methods.**

Pet Bottles Blend/ Preparation

Polyethylene Terephthalate (PET) waste bottles were subjected to an extensive cleaning process to remove impurities, such as sand, dirt, and other non-plastic materials. Following this, the PET bottles were washed with clean water and then left to air dry under the sun for three days. Once they were dry, the bottles were cut into small pieces and further processed with a Silver crest 8500watts blender to produce even finer particles, which increased their surface area to facilitate easier dissolution in the solvent.

C. Extraction of Chitin

The snail shells were collected, organized, and thoroughly cleaned with fresh water, followed by multiple rinses with deionized water to eliminate any flesh, sand, and organic residues like debris that could interfere with the production processes. The samples were then left to dry in the sun for two days to reduce moisture content and subsequently dried in a hot air oven at 80 °C for four hours. After drying, the shells were crushed using a pestle and mortar, ground into a fine powder, and passed through a 150 µm sieve to ensure effective chemical treatment. To accomplish demineralization, 1000 g of snail shell powder was weighed using an analytical balance and mixed with 500 ml of hydrochloric acid (HCl) in a 1:2 g/ml (w/v) proportion. This combination was vigorously stirred and maintained at room temperature (32 °C) for a duration of 24 hours. Subsequently, it was thoroughly washed with distilled water until it reached a neutral pH and then filtered through a 150 µm sieve. The remaining substance was rinsed with deionized water and dried in a tray dryer at 80°C for 24 hours to yield demineralized chitin.

The process of deproteinization involved treating the demineralized chitin with 500 ml of NaOH, maintaining a constant stir at 90 °C for a duration of 2 hours to effectively remove proteins. Following this, the mixture was passed through a 150 µm sieve and subsequently filtered. The resulting filtrate was washed with distilled water for 30 minutes until it reached a neutral pH. Finally, the deproteinized material was dried in an oven set at 80°C for 24 hours, resulting in the production of crude chitin.

D. Production of Chitosan

A 50% (w/v) Sodium Hydroxide (NaOH) solution was introduced to the chitin for deacetylation, and the mixture was heated at 100 °C in a water bath for 3 hours. The chitin was then thoroughly rinsed with distilled water to eliminate any remaining Sodium Hydroxide. Subsequently, the samples were dried in an oven set at 120 °C for 4 hours. The chitosan was further processed by grinding and sieving into a powder to achieve a particle size of 0.063 µm.

E. Preparation of the dope solution

In an empty beaker, 10 g of Polyethylene terephthalate (PET) was weighed and added. Subsequently, 25 ml of

trifluoroacetic acid (TFA) was introduced to the PET in the beaker. The mixture was then heated on a mantle at 60 °C with vigorous stirring until a gelatinous dope was formed, which was then left to cool. Once cooled, 5 g of chitosan, derived from snail shells, was measured and slowly incorporated into the PET/TFA dope solution in the same beaker. The mixture was continuously stirred until the chitosan completely dissolved, resulting in a homogeneous dope solution.

F. Casting of membrane

The membrane fabrication process utilized the solution casting method outlined by (Sahu et al., 2024) Abdullah et al. (2016). Polymer dope solution blends were poured into a 30 cm diameter glass Petri dish (Pyrex, England). The solution was carefully added to the dish and allowed to dry over a period of three days, ensuring the formation of a solid polymer membrane cast. The resulting membranes had an average thickness of about 0.25 mm. The membrane underwent solvent evaporation in atmospheric conditions for five days. Afterward, the flat circular membrane sheet was extracted from the glass Petri dish and placed in a water bath filled with distilled water at 55 °C for 30 minutes to remove the solvents. It was then dried in an oven at 80 °C for three hours until a constant weight was achieved, as measured by an analytical balance (Scout Pro, Ohaus, England).

Figure 1. Illustration of the membrane fabrication Process.

2.3 Characterization methods

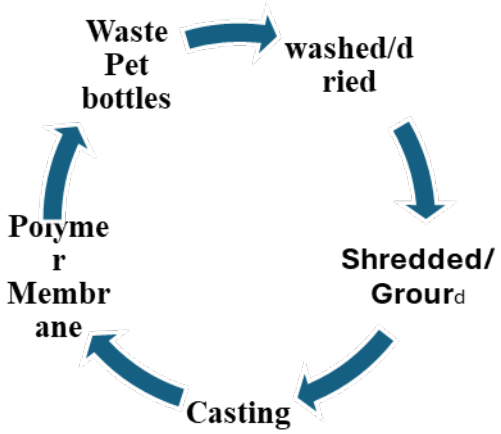

In other to understand the structure, composition, and functionality of membranes, characterization methods are vital for optimizing their performance (Sahu et al., 2024). This study employed the following characterization methods:

Fourier transform infrared (FTIR), Scanning Electron Microscopy/Energy Dispersive X-ray Spectroscopy (SEM/EDX), Thermogravimetric Analysis (TGA)/Differential Thermal Analysis (DTA).

To assess the alterations in functional groups within the fabricated polymer membrane sample, FTIR analysis was performed. This test adhered to the ASTM E168-16 standard. The spectra were captured over a frequency range of 500 cm-1 to 4000 cm-1 using an FT-IR spectrometer (Infrared spectrometer Variant 660 MidIR Dual MCT/DTGS Bundle with ATR), equipped with a detector set at a resolution of 4 cm-1 and conducting 200 scans per sample.

To assess the shape and morphology of the fabricated membrane sample, Scanning Electron Microscopy/Energy Dispersive X-ray Spectroscopy (SEM-EDX) (Hitachi SU 3500, Tokyo, Japan) was utilized. This combination of SEM and EDX allows for the elemental analysis of the membrane material, providing insights into the chemical composition and distribution of elements on the membrane's surface. These techniques are essential for comprehending the physical and chemical characteristics of polymer membranes, which have a direct impact on their filtration performance (Barzegar et al., 2021; Mandal et al., 2018). Energy Dispersive X-ray Spectroscopy (EDX) analysis was used to examine the physical morphology of sample surfaces and to analyze the element compositions.

In this research, a Q50 TGA from Shimadzu Instruments (Shimadzu TGA - Q50 thermo-balance) thermal analyzer was employed for thermogravimetric analysis. Thermogravimetric/differential thermal analysis (TGA/DTA) is a technique that evaluates the mass changes of a sample as it is subjected to varying temperatures. This method was utilized to investigate the thermal properties of the polymer membrane. The study adhered to the ASTM E2105-16 standard to assess the thermal and oxidative stability of the membrane's characteristics. These evaluations are primarily conducted to determine the thermal and/or oxidative stability of materials, as well as their compositional attributes(Martincic et al., 2024). This approach is effective for examining materials that experience mass changes due to decomposition, oxidation, or the evaporation of volatiles such as moisture(Cao & Mu, 2014).

III. Results and Discussion.

A. Ftir Analysis

Figure 2 illustrates the reflected spectra of the constructed membrane, revealing the presence of various functional groups within it. The peak at 2703.11 cm^{-1} is associated with the O-H stretching vibration band, which is linked to the vibrations caused by intermolecular hydrogen bonding in polymeric compounds, alcohols, phenols, and carboxylic acids on the carbon surface (Giubertoni et al., 2020; Palumbo et al., 2021). The peak at 2502.64 cm^{-1} results from C-H stretching vibration. The 1712 cm^{-1} vibration bands suggest a weak PET marker or are weakly expressed or overlapped, indicating esters C=O stretching of PET, typically the most prominent PET band (Zhu et al., 2003), its reduction in this spectrum implies a low PET fraction or reduced crystallinity (Onyishi & Oluah, 2020) () or partial overlap with nearby bands from chitosan. The peaks at 1531 cm^{-1} correspond to the N-H stretching vibration bands of amide (Patel et al., 2025; Suneetha, 2018).

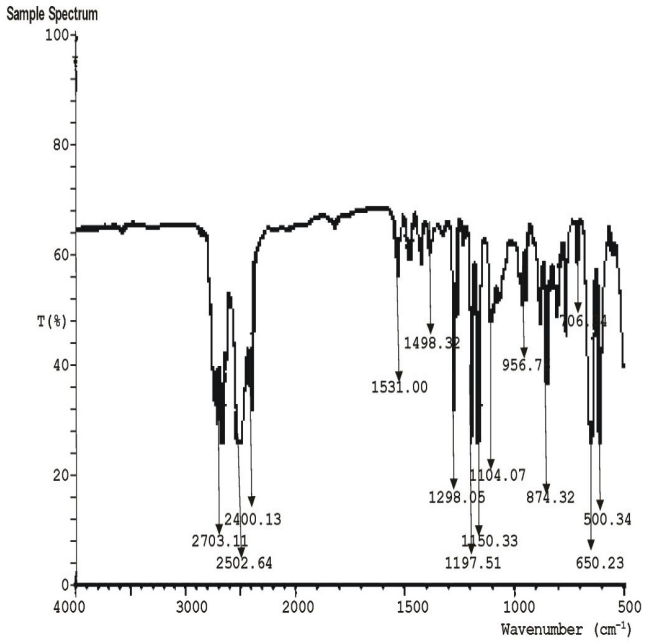

Figure 2. FTIR Spectra of PET/Chitosan Membrane

The peaks at 1298.05 cm-[1] indicate N-H bending vibrations, aligning with Dambuza et al (2025), who reported a similar peak at 1295 cm-[1] designated as NH2 stretching vibrations of amines. The 1197.51 cm-[1] bandwidth also corresponds to asymmetric and symmetric S-O sulfonated stretching groups found in polymer and petroleum product. Giubertoni et al (2020) also identifying the same peak at 1160 cm-[1]. The bandwidth at 1104.07 cm-[1] indicates C(CH2) stretching vibrations of alkanes, while the peak at 956.7 cm-1 is attributed to C-O stretching of aromatic esters as present in the PET backbone (). The peak at 874.32 cm-[1] is linked to the C-N stretching vibrations of amides, while the peak at 703.34 represents the C-NH3 stretching vibration of primary aliphatic amines ()(Yang et al., 2016). (Hie et al., 2015)The peaks at 650.23 cm-1 and 500.34 cm-[1] are attributed to the C-C and C-H stretching vibrations and out-of-plane bending vibrations, respectively, of alkanes (Esenturk & Walker, 2006; Smith, 1999).

The detection of PET-specific aromatic bands at 1498.32 cm-[1] and 874.82 cm-[1], along with the chitosan amide II band at 1531.00 cm-[1] and saccharide C–O/C–O–C bands within the 1150–1060 cm-[1] range, notably at 1104.07 cm-[1], indicates the incorporation of both components into the membrane (Nicolle et al., 2021), as also highlighted in other studies (Abubakar et al., 2021) (Kızılkaya & Kaya, 2024). The quantitative analysis of the amide II intensity shift and the broadening in the 1150–1060 cm-[1] range clearly indicates that the 1104.07 cm-[1] envelope is associated with hydrogen bonding between chitosan N–H/O–H donors and PET carbonyl acceptors. This is a common compatibilization mechanism in PET–polysaccharide blends. The positioning of the bands and the interactions involving hydrogen bonding with the PET ester C=O typically result in a weakening and a slight shift of the 1712–1725 cm-1 bandwidth to a lower wavenumber, approximately 1710 cm-[1], along with a decrease in its relative intensity (P. Chen et al., 2021; Decato et al., 2022; Prasad et al., 2011) Meanwhile, the chitosan amide II band moves towards 1530 cm-[1]. The 1531 cm-[1] observed in this study aligns with this trend.

The interaction at the interface, as evidenced by spectral shifts and the broadening of the band envelope, suggests the presence of hydrogen bonding between polymers rather than covalent transamidation(Haugstad et al., 2015; Sahni et al., 2008). The spectra did not reveal any new bands indicative of imide or amide carbonyls beyond those of the native chitosan amide (Elhaes et al., 2024; Zakaria et al., 2012).

Figure 1 depicts the interactions between PET and chitosan as observed in their spectra. PET is known for its characteristic C=O stretching, typically found in the 1710–1730 cm^{-1} range, which is shown here as a subtle band at 1710 cm-1, along with aromatic C=C stretching bands.(Awad & Khalaf, 2018) In PET and chitosan blends, any shifts or broadening in the carbonyl or amide bands, as well as changes in the intensity of the OH/NH region, may indicate hydrogen bonding interactions between the ester carbonyl groups of PET and the hydroxyl and amino groups of (Giubertoni et al, 2020). These intermolecular interactions can somewhat enhance the compatibility between the two phases and affect both the mechanical properties and water absorption. Although the hydrogen bonding is weak, it is often enough to stabilize a semi-interpenetrating network, which is consistent with SEM observations showing co-continuous dense domains rather than significant macroscopic-phase separation (Espíndola-González et al., 2011; Paul et al., 2024; Sun et al., 2022).

From the above analysis, the overall spectrum corroborates a PET–chitosan composite membrane in which both polymer backbones are retained and interact via hydrogen bonding.

B. SEM/EDX Analyis

Figure 3 presents the SEM/EDX micrograph, which provides a view of the surface morphology and elemental composition of the created polymer membrane. The Scanning Electron Microscopy (SEM) image, captured at a 50000x magnification with a 500 nm scale bar, reveals the complex surface characteristics of the polymer membrane (Davies et al., 2022). The membrane's surface seemed to be quite compact and consistent, showing no visible large pores or notable gaps. The lack of prominent large pore structures implies a compact surface morphology, suggesting a densely packed top-layer membrane (Kusumocahyo et al., 2021). (Primc and Mozetič, 2022) The surface characteristics can be linked to chitosan's hydrophilic nature and its limited compatibility with the more hydrophobic PET matrix (Lopes-Da-Silva et al., 2009; Vafakish & Wilson, 2019).

The remaining mineral content from the snail shell, primarily $CaCO_3$, functions as a micro-filler and may act as nucleation sites for pore formation and interfacial defects. (Stel'Makh et al., 2022) This phenomenon has been observed in similar systems where $CaCO_3$ or other inorganic fillers are incorporated into polymer matrices. This effect has also been

 ISSN: **3107-6513**

documented by other researchers (Jafari et al, 2016; Malkoske, et al, 2025)

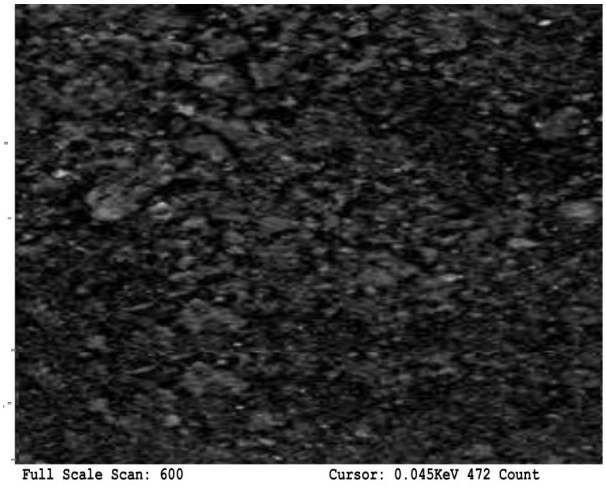

Figure 3.SEM Image of PET/Chitosan Membrane

The lack of large macrovoids and the presence of fine pores and domain (Szopa et al., 2025) suggest that the casting conditions favored a relatively controlled, diffusion-limited phase separation rather than an instant demixing typical of highly porous ultrafiltration membranes, a (Al-Musawy et al., 2025; M. Chen et al., 2022). According to the SEM findings, the addition of chitosan derived from snail shells alters the morphology of the PET membrane, transforming it from a dense and relatively smooth structure into a more microporous and roughened composite. These modifications are anticipated to affect the membrane's permeability, surface hydrophilicity, and fouling characteristics, as has been observed in other PET and chitosan-based blended membranes (Jeon et al., 2016; Pintilie et al., 2017).

C. **EDX Analysis**

Energy Dispersive X-ray (EDX) analysis, as shown in Figure 4, provides the elemental composition of the analyzed fabricated membrane. The peaks in the spectrum correspond to the characteristics X-ray emissions from specific elements. A very strong peak of carbon (C) was observed at approximately 1.5KeV, indicating that carbon is the most abundant element present (Hossain, 2013). This aligns with the polymeric characteristics of the membrane, which consists of PET and chitosan. A pronounced peak is observed for oxygen (O) at approximately 3.8KeV, signifying a significant presence of oxygen. Both PET (polyethylene terephthalate) and chitosan, which have oxygen-containing functional groups, are anticipated to exhibit this characteristic.

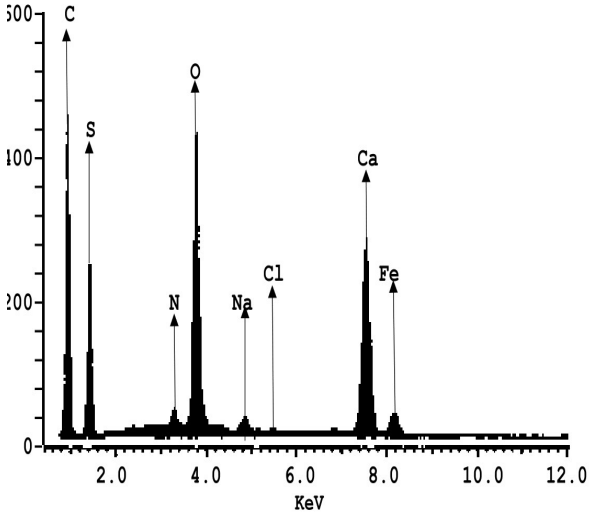

Figure 4.EDX Spectrum of PET/Chitosan Membrane

A significant calcium (Ca) peak was observed at around 7.6KeV. The notable presence of a significant amount of calcium is particularly interesting, considering that chitosan was derived from snail shells, which are mainly made up of calcium carbonate ($CaCO_3$) (). This indicates that some calcium compounds might still be present in the chitosan or the final membrane (Kato, 2000). This residual inorganic material has (Karthick Rajan et al., 2023) been widely documented by numerous authors. Among the minor elements detected, nitrogen (N) shows a small peak around 4.9KeV, this element is a typical component of chitosan (Gorgieva et al., 2021), indicating its presence in the membranes. Additionally, sulfur (S) appears with a moderate peak at approximately 1.7KeV, the sulfur detected might stem from leftover chemicals used during synthesis or from impurities in the initial materials. Sodium (Na) was also observed at a minor peak around 4.9 KeV, potentially originating from processing agents or contamination from the environment. Chlorine (Cl) was identified at a minor peak around 5.6KeV, which might suggest the presence of chlorine-containing compounds left over from the synthesis process. An intermediate peak for iron (Fe) appeared at about 8.2KeV, implying that iron was probably an impurity, potentially originating from the raw materials or the equipment used during fabrication (Palanisamy et al., 2023). The membranes made from PET and chitosan also exhibited peaks for N and Ca, indicating the successful incorporation of chitosan and remaining mineral phases from snail shells, which has been previously documented (Jafari Sanjari & Asghari, 2016; Lakshmi et al., 2024; Nikita et al., 2025). The detection of Ca aligns with the partial retention of $CaCO_3$ derived from snail shells during the processes of demineralization and deacetylation, similar observations have been made for chitosan sourced from both crustacean and snail shells, where residual calcium carbonate remains even after acid treatment, functioning as an inherent inorganic filler (Karim et al., 2024)

Elemental mapping reveals that nitrogen and calcium are primarily concentrated within the chitosan-rich areas identified in SEM, verifying that these morphological characteristics are associated with regions abundant in biopolymers and mineral phases, rather than mere voids. Similar distributions have been observed in chitosan/$CaCO_3$ hybrid materials and chitosan membranes filled with bioceramics, where calcium-containing particles are dispersed and occasionally partially surrounded by chitosan (Nikita et al.,2025; Zhu et al., 2003). From a functional stand point, the presence of N-rich chitosan at or near the membrane surface has important implications (Dambuza et al., 2025) (). Chitosan's positively charged amino groups can provide antimicrobial effects and improve the adsorption of negatively charged pollutants, dyes, and metal ions(Babaei-Ghazvini et al., 2021; Su et al., 2022; Xing et al., 2014) (Rinaudo, 2006; Crini & Badot, 2008). The Ca-containing mineral phase can contribute to mechanical reinforcement and modify surface energy, which may improve dimensional stability and influence fouling and scaling behavior. (Malkoske et al., 2025)

EDX analysis verified the presence of nitrogen and calcium in the composite membranes, clearly indicating the integration of chitosan and the remaining mineral phases from the snail shells. The combined use of PET and snail shell waste illustrates an effective and sustainable method for creating value-added functional materials within a circular economy framework.

D. **TGA/DTA**.

Figure 5 illustrates the TGA profile of the PET/chitosan membrane, revealing several distinct phases of mass reduction as the temperature ranges from 200 °C to 900 °C in a nitrogen atmosphere. Since the initial temperature was set at 200 °C, there was no notable loss of mass at the beginning (Călin et al., 2024), only a minor fluctuation that aligns with the lack of low-temperature volatile substances following prior drying. In the case of chitosan, the initial phase at low temperatures is not detected here because the experiment begins at 200°C. The subsequent significant mass reduction is associated with the thermal degradation of the chitosan phase(Hong et al., 2007). The process of chitosan depolymerization and decomposition starts around 300–350°C, involving the dehydration of saccharide rings, the cleavage of glycosidic bonds, and the formation of volatile fragments such as CO_2, NH_3, and small organic compounds (Sari et al., 2021).

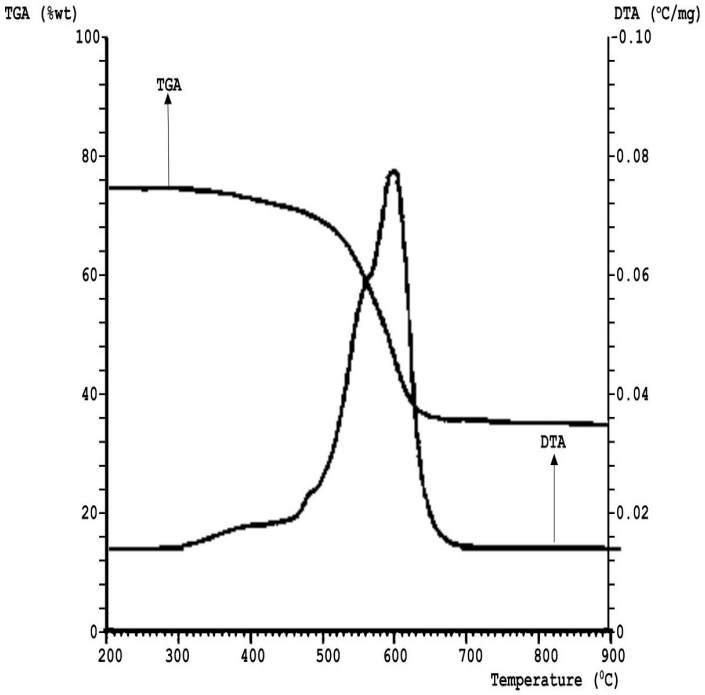

Figure 5. Thermal Gravimetric profile of PET/Chitosan Membrane

The primary breakdown or degradation of the PET backbone begins between 350 and 400 °C and can extend to temperatures of 500 to 550 °C, influenced by factors such as molecular weight, crystallinity, and the presence of additives (Chowdhury & Wang, 2023; Schubert et al., 2024; Thomsen et al., 2023).This phase signifies the primary event of mass loss, characterized by chain scission, the breaking of ester bonds, and the emission of flammable degradation products such as hydrocarbons, CO, and CO_2 (Costache et al., 2006). The degradation of PET is marked by a sharp drop in the TGA curve. The degradation of PET began at 500 °C in this study, consistent with values found in the literature due to the presence of calcium carbonate, which serves as a filler, along with some other additive (Brott et al., 2021; Chowdhury and Wang, 2023; Then et al., 2016).

Char formation and a gradual reduction in mass were observed beyond roughly 550 °C, with the rate of mass loss diminishing as the TGA curve gradually approached a plateau at higher temperatures, ranging from about 650 °C to 900 °C. The residual mass within this temperature range is mainly associated with thermally stable carbon-rich char and inorganic substances from the snail shell, such as CaO or similar mineral derivatives, as well as any charred organic residues (Deodhar et al., 2010). Chitosan often aids in char formation, which can improve flame retardancy and thermal resistance. (Xu et al., 2019) The composite polymer membrane demonstrated a multi-phase degradation pattern illustrative of a composite PET/chitosan systems, as evidenced by the TGA curve, which showed the combined influence of both polymer components.

The degradation temperatures and thermal stability of the membrane are primarily indicated by the onset degradation temperature, approximately 450°C, and the temperature at which the degradation rate is highest, around 600°C (Tmax) (Gubanova et al., 2021). In the PET/chitosan composite analyzed in this research, the Tonset was observed at 450°C, attributed to the presence of additives that led to an increase in the Tonset. It has been observed that chitosan modify the PET degradation phase due to interactions such as hydrogen bonding between the ester groups of PET and the amino or hydroxyl groups of chitosan (Thomsen et al,2023), which may affect chain mobility and thermal scission pathways. The char yield, or residual mass, between 650°C and 900°C is an essential factor in assessing the performance at high temperatures and the potential flame-retardant characteristics.

Conversely, the presence of chitosan and inorganic elements from snail shell–based precursors boosts the formation of char.The detection of a non-zero residue in the membrane sample at temperatures between 650°C and 900°C suggests that chitosan and inorganic residues contribute positively to the char yield. This increase in residue implies improved resistance to complete volatilization, which can be beneficial for applications that require thermal stability and reduced flammability (Mapossa et al., 2024; Mhlabeni et al., 2025; Sui et al., 2020).

The DTA curve, recorded alongside the TGA, is depicted in **Figure 5** above, offering insights into the endothermic and exothermic thermal events occurring during the heating process. The polymer membrane sample displayed several distinct characteristics. In the temperature range of 200–350 °C, distinct intermediate-temperature phenomena occur during the breakdown of chitosan. As chitosan undergoes decomposition, the DTA signal reveals overlapping endothermic and faint exothermic characteristics. The endothermic response is linked to the processes of bond breaking and volatilization, while the exothermic portions might be related to crosslinking, aromatization, and char formation. This complexity is characteristic of materials based on polysaccharides, such as chitin. (Levchik & Weil, 2004; Vasilev et al., 2019)

When temperatures rise between 350 and 600 °C, a clear endothermic peak linked to the breakdown of PET appears as a prominent endothermic DTA peak, corresponding with the fastest stage of mass reduction on the TGA curve, this peak represents the energy required to break ester bonds and vaporize the degradation product. Incorporating chitosan and inorganic substances can cause slight alterations in the position and strength of the peak, as they influence the overall energy dynamics and heat transfer (Radu et al., 2023; Tamburaci and Tihminlioglu, 2017). The DTA results generally align with the multi-step degradation pattern observed in TGA, confirming that the composite membrane experiences thermal transitions related to the PET and chitosan components.

The findings from the thermal analysis have several consequences for the practical application of PET/chitosan membranes created from PET waste and snail shells: The composite maintains thermal stability at temperatures ranging from 200 to 300 °C before notable chitosan degradation occurs, which is more than adequate for most water treatment and low-temperature separation applications. The significant PET degradation occurring above 350 °C suggests that the membrane is unsuitable for extremely high-temperature settings. However, the typical operating conditions for the fabricated membrane are well below these thresholds. The increased formation of char due to the presence of chitosan and inorganic residues indicates a better resistance to total mass loss and may provide some level of flame-retardant properties compared to unaltered PET.

Therefore, the TGA/DTA findings indicate that transforming PET waste and chitosan derived from snail shells into composite membranes results in materials that possess adequate thermal stability, significant char formation, and the potential for additional functional advantages.

IV. Conclusion

The PET/chitosan composite membrane showed characteristic PET bands (ester C=O stretching and aromatic ring vibrations) were present along with modified chitosan bands. The broad –OH/–NH band, amide region, and C–O–C/C–O bands attributable to chitosan were observable but with reduced intensity and slight shifts, indicating the coexistence of both polymers and intermolecular interactions, mainly hydrogen bonding, between chitosan and PET. These spectral changes demonstrate that chitosan is effectively incorporated into the PET membrane and that its functional groups remain available, albeit in a different microenvironment. SEM analysis revealed that the incorporation of snail-shell-derived chitosan transforms the membrane morphology into a dense structure with increasing roughness and domain formation. EDX confirmed the presence of nitrogen and calcium in the composite membranes, providing clear evidence of chitosan incorporation and residual biogenic mineral phases from snail shells. TGA/DTA analysis under nitrogen up to 900 °C revealed a multi-step degradation process with overlapping degradation events of chitosan and PET backbones and enhanced residual mass at high temperatures, indicative of char formation and inorganic residue from snail shell origin.
These findings demonstrate that snail shell–derived chitosan can be effectively incorporated into PET waste membranes without compromising their thermal stability in common operating ranges. Instead, the composite gains added value through improved high-temperature residue formation and the introduction of bio-based functional groups. When combined with structural (SEM) and chemical (FTIR) evidence, the results support the suitability of these membranes for potential applications especially where both physical filtration and adsorptive removal of contaminants are desired. The dual utilisation of PET and snail shell wastes demonstrates a viable, sustainable pathway for producing value-added functional materials within a circular economy framework

Acknowledgement: This research was funded by the Tertiary Education Trust Fund (TETFUND) through the Auchi Polytechnic Centre for Research and Innovation and

Development (CRID). We are sincerely grateful for the assistance

Conflicts of Interest: The authors declare no conflict of interest.

V. References

Aare, D. F. F., Ogiri, T. O., Tekaron, D. O. A., & Ntor, G. G. (2024). Strategic management of plastic pollution in Nigeria: Balancing best approaches. *International Journal of Civil Law and Legal Research*, *4*(1), 05–14. https://doi.org/10.22271/civillaw.2024.v4.i1a.58

Abubakar, J., Pasaoglulari Aydinlik, N., & Edo, G. (2021). Phytochemical and GCMS analysis on the ethanol extract of Foeniculum Vulgare and Petroselinum crispum leaves. *International Journal of Chemistry and Technology*, *5*(2), 117–124. https://doi.org/10.32571/ijct.911711

Al-Musawy, W. K., Ibraheem, B. M., Darwesh, T. M., Al-Furaiji, M. H., Awad, M., & Alsalhy, Q. F. (2025). Synthesis and Performance of Polysulfone-Chitosan Ultrafiltration Membranes for Humic Acid Removal. *Desalination and Water Treatment*, *321*, 100939. https://doi.org/10.1016/j.dwt.2024.100939

Awad, S. A., & Khalaf, E. M. (2018). Improvement of the chemical, thermal, mechanical and morphological properties of polyethylene terephthalate–graphene particle composites. *Bulletin of Materials Science*, *41*(3). https://doi.org/10.1007/s12034-018-1587-1

Babaei-Ghazvini, A., Korber, D. R., & Acharya, B. (2021). Antimicrobial Biodegradable Food Packaging Based on Chitosan and Metal/Metal-Oxide Bio-Nanocomposites: A Review. *Polymers*, *13*(16), 2790. https://doi.org/10.3390/polym13162790

Barzegar, H., Masteri-Farahani, M., Shahsavarifar, S., & Vatanpour, V. (2021). Peroxopolyoxometalate nanoparticles blended <scp>PES</scp> membrane with improved hydrophilicity, anti-fouling, permeability, and dye separation properties. *Journal of Applied Polymer Science*, *138*(31), 50764. https://doi.org/10.1002/app.50764

Brott, S., Schwarz, J., Pfaff, L., Schuricht, J., Böttcher, D., Badenhorst, C. P. S., Bornscheuer, U. T., & Wei, R. (2021). Engineering and evaluation of thermostable IsPETase variants for PET degradation. *Engineering in Life Sciences*, *22*(3–4), 192–203. https://doi.org/10.1002/elsc.202100105
Călin, C., Győrgy, R., Sîrbu, E.-E., Popovici, D. R., Banu, I., & Tănase, M. (2024). A Thermogravimetric Analysis of Biomass Conversion to Biochar: Experimental and Kinetic Modeling. *Applied Sciences*, *14*(21), 9856. https://doi.org/10.3390/app14219856

Cao, Y., & Mu, T. (2014). Comprehensive Investigation on the Thermal Stability of 66 Ionic Liquids by Thermogravimetric Analysis. *Industrial & Engineering Chemistry Research*, *53*(20), 8651–8664. https://doi.org/10.1021/ie5009597

Chen, H. L., Chong, S., Lechner, A. M., Gibbins, C., Nath, T. K., & Foo, V. (2021). The plastic waste problem in Malaysia: management, recycling and disposal of local and global plastic waste. *SN Applied Sciences*, *3*(4). https://doi.org/10.1007/s42452-021-04234-y

Chen, M., Cui, Z., Zhou, Y., Wang, Z., Xing, W., & Sun, Q. (2022). Preparation of PVDF membrane via synergistically vapor and non-solvent-induced phase separation. *Applied Water Science*, *12*(7). https://doi.org/10.1007/s13201-022-01683-7

Chen, P., Xie, F., Tang, F., & Mcnally, T. (2021). Influence of plasticiser type and nanoclay on the properties of chitosan-based materials. *European Polymer Journal*, *144*, 110225. https://doi.org/10.1016/j.eurpolymj.2020.110225

Chowdhury, T., & Wang, Q. (2023). Study on Thermal Degradation Processes of Polyethylene Terephthalate Microplastics Using the Kinetics and Artificial Neural Networks Models. *Processes*, *11*(2), 496. https://doi.org/10.3390/pr11020496

Costache, M. C., Wilkie, C. A., Heidecker, M. J., Manias, E., & Wang, D. (2006). The thermal degradation of poly(methyl methacrylate) nanocomposites with montmorillonite, layered double hydroxides and carbon nanotubes. *Polymers for Advanced Technologies*, *17*(4), 272–280. https://doi.org/10.1002/pat.697

Dambuza, A., Mokolokolo, P. P., Makhatha, M. E., & Sibeko, M. A. (2025). Chitosan-Based Materials as Effective Materials to Remove Pollutants. *Polymers*, *17*(18), 2447. https://doi.org/10.3390/polym17182447

Davies, T. E., Dummer, N. F., Bessette, S., Patience, G. S., Gauvin, R., & Li, H. (2022). Experimental methods in chemical engineering: Scanning electron microscopy and<scp>X</scp>-ray ultra-microscopy—<scp>SEM</scp>and<scp>XuM</scp>. *The Canadian Journal of Chemical Engineering*, *100*(11), 3145–3159. https://doi.org/10.1002/cjce.24405

Decato, D. A., Sun, J., Boller, M. R., & Berryman, O. B. (2022). Pushing the limits of the hydrogen bond enhanced halogen bond—the case of the C–H hydrogen bond†. *Chemical Science*, *13*(37), 11156–11162. https://doi.org/10.1039/d2sc03792k
Deodhar, S., Costache, M. C., Fan, Q., Patra, P. K., Wilkie, C. A., Dembsey, N. A., & Shanmuganathan, K. (2010). Calcium carbonate and ammonium polyphosphate-based flame retardant composition for polypropylene. *Journal of Applied Polymer Science*, *120*(3), 1866–1873. https://doi.org/10.1002/app.32510

Elhaes, H., Ezzat, H. A., Ibrahim, A., Samir, M., Refaat, A., & Ibrahim, M. A. (2024). Spectroscopic, Hartree–Fock and DFT study of the molecular structure and electronic properties of

functionalized chitosan and chitosan-graphene oxide for electronic applications. *Optical and Quantum Electronics*, *56*(3). https://doi.org/10.1007/s11082-023-05978-0

Esenturk, O., & Walker, R. A. (2006). Surface vibrational structure at alkane liquid/vapor interfaces. *The Journal of Chemical Physics*, *125*(17), 174701. https://doi.org/10.1063/1.2356858

Espíndola-González, A., Castaño, V. M., Datashvili, T., Fernández-Escobar, F., Martínez-Hernández, A. L., Brostow, W., & Velasco-Santos, C. (2011). Natural-Synthetic Hybrid Polymers Developed via Electrospinning: The Effect of PET in Chitosan/Starch System. *International Journal of Molecular Sciences*, *12*(3), 1908–1920. https://doi.org/10.3390/ijms12031908

Giubertoni, G., Sofronov, O. O., & Bakker, H. J. (2020). Effect of intramolecular hydrogen-bond formation on the molecular conformation of amino\xa0acids. *Communications Chemistry*, *3*(1). https://doi.org/10.1038/s42004-020-0329-7

Gorgieva, S., Osmić, A., Hribernik, S., Božič, M., Svete, J., Hacker, V., Wolf, S., & Genorio, B. (2021). Efficient Chitosan/Nitrogen-Doped Reduced Graphene Oxide Composite Membranes for Direct Alkaline Ethanol Fuel Cells. *International Journal of Molecular Sciences*, *22*(4), 1740. https://doi.org/10.3390/ijms22041740

Gubanova, G. N., Petrova, V. A., Kononova, S. V., Popova, E. N., Smirnova, V. E., Bugrov, A. N., Klechkovskaya, V. V., & Skorik, Y. A. (2021). Thermal Properties and Structural Features of Multilayer Films Based on Chitosan and Anionic Polysaccharides. *Biomolecules*, *11*(5), 762. https://doi.org/10.3390/biom11050762

Haugstad, K., Draget, K., Nordgård, C., Maurstad, G., Adl, P., Håti, A., Stokke, B., Sletmoen, M., & Dias, R. (2015). Direct Determination of Chitosan–Mucin Interactions Using a Single-Molecule Strategy: Comparison to Alginate–Mucin Interactions. *Polymers*, *7*(2), 161–185. https://doi.org/10.3390/polym7020161

Hie, L., Fine Nathel, N. F., Liu, P., Yang, Y.-F., Baker, E. L., Houk, K. N., Hong, X., Shah, T. K., & Garg, N. K. (2015). Conversion of amides to esters by the nickel-catalysed activation of amide C-N bonds. *Nature*, *524*(7563), 79–83. https://doi.org/10.1038/nature14615

Hong, P., Li, S., Yang, L., Ou, C., Li, C., & Zhang, C. (2007). Thermogravimetric analysis of chitosan. *Journal of Applied Polymer Science*, *105*(2), 547–551. https://doi.org/10.1002/app.25920

Hossain, M. A. (2013). Synthesis of Carbon Nanoparticles from Kerosene and their Characterization by SEMÆDX, XRD and FTIR. *American Journal of Nanoscience and Nanotechnology*, *1*(2), 52. https://doi.org/10.11648/j.nano.20130102.12

Jafari Sanjari, A., & Asghari, M. (2016). A Review on Chitosan Utilization in Membrane Synthesis. *ChemBioEng Reviews*, *3*(3), 134–158. https://doi.org/10.1002/cben.201500020

Jeon, S., Kato, N., Matsuyama, H., Okamura, R., Hasegawa, S., Rajabzadeh, S., & Ishigami, T. (2016). The Effect of Membrane Material and Surface Pore Size on the Fouling Properties of Submerged Membranes. *Water*, *8*(12), 602. https://doi.org/10.3390/w8120602

Karim, M. M., Lasker, T., Sahin, M. A. Z., Hossain, M. S., & Saputra, H. A. (2024). Low-Cost Production of Chitosan Biopolymer from Seafood Waste: Extraction and Physiochemical Characterization. *Journal of Research Updates in Polymer Science*, *13*, 17–26. https://doi.org/10.6000/1929-5995.2024.13.03

Karthick Rajan, D., Zhang, S., Ramu Ganesan, A., Divya, D., Kumar, R., Rajarajeswaran, J., Kandasamy, S., & Mohan, K. (2023). β-Chitin and chitosan from waste shells of edible mollusks as a functional ingredient. *Food Frontiers*, *5*(1), 46–72. https://doi.org/10.1002/fft2.326

Kato, T. (2000). Polymer/Calcium Carbonate Layered Thin-Film Composites. *Advanced Materials*, *12*(20), 1543–1546. https://doi.org/10.1002/1521-4095(200010)12:20<1543::aid-adma1543>3.0.co;2-p

Kibria, M. G., Masuk, N. I., Safayet, R., Nguyen, H. Q., & Mourshed, M. (2023). Plastic Waste: Challenges and Opportunities to Mitigate Pollution and Effective Management. *International Journal of Environmental Research*, *17*(1). https://doi.org/10.1007/s41742-023-00507-z

Kızılkaya, P., & Kaya, M. (2024). Chitosan/TiO2/Rosmarinic Acid Bio-Nanocomposite Coatings: Characterization and Preparation. *Journal of Composites Science*, *9*(1), 2. https://doi.org/10.3390/jcs9010002

Kusumocahyo, S. P., Ambani, S. K., & Marceline, S. (2021). Improved permeate flux and rejection of ultrafiltration membranes prepared from polyethylene terephthalate (PET) bottle waste. *Sustainable Environment Research*, *31*(1). https://doi.org/10.1186/s42834-021-00091-x

Lakshmi, D. S., Ravindran, L., Mary, P. J. M., Rathika, G., Sreekala, M. S., & Munisamy, S. (2024). Valorization of Crustacean Shells: Preparation, Characterization, and Chemical Modification of Nano-Chitin Biopolymer Membrane for Application in Water Purification. *Waste and Biomass Valorization*, *15*(11), 6067–6090. https://doi.org/10.1007/s12649-024-02601-5

Levchik, S. V., & Weil, E. D. (2004). A review on thermal decomposition and combustion of thermoplastic polyesters. *Polymers for Advanced Technologies*, *15*(12), 691–700. https://doi.org/10.1002/pat.526

Lopes-Da-Silva, J. A., Veleirinho, B., & Delgadillo, I. (2009). Preparation and Characterization of Electrospun Mats Made of PET/Chitosan Hybrid Nanofibers. *Journal of Nanoscience and*

Nanotechnology, *9*(6), 3798–3804. https://doi.org/10.1166/jnn.2009.ns70

Lorenzi, L., Reginato, B. C., Dantas, D. V., & Mayer, D. G. (2020). Plastic floating debris along a summer-winter estuarine environmental gradient in a coastal lagoon: how does plastic debris arrive in a conservation unit? *Environmental Science and Pollution Research*, *27*(8), 8797–8806. https://doi.org/10.1007/s11356-020-07708-5

Malkoske, T. A., Cai, Y.-H., Bone, S. E., & Schäfer, A. I. (2025). Calcium-organic matter fouling in nanofiltration: Synchrotron-based X-ray fluorescence and absorption near-edge structure spectroscopy for speciation. *Water Research*, *272*, 122938. https://doi.org/10.1016/j.watres.2024.122938

Mandal, M., Secanell, M., Valls, A., & Gangnus, N. (2018). Analysis of Inkjet Printed Catalyst Coated Membranes for Polymer Electrolyte Electrolyzers. *Journal of The Electrochemical Society*, *165*(7), F543–F552. https://doi.org/10.1149/2.1101807jes

Mapossa, A. B., Dos Anjos, E. G. R., & Sundararaj, U. (2024). Boosting Flame Retardancy of Polypropylene/Calcium Carbonate Composites with Inorganic Flame Retardants. *Materials (Basel, Switzerland)*, *17*(18), 4553. https://doi.org/10.3390/ma17184553

Martincic, M., Sandoval, S., Oró-Solé, J., & Tobías-Rossell, G. (2024). Thermal Stability and Purity of Graphene and Carbon Nanotubes: Key Parameters for Their Thermogravimetric Analysis (TGA). *Nanomaterials (Basel, Switzerland)*, *14*(21), 1754. https://doi.org/10.3390/nano14211754

Mhlabeni, T. L., Mhike, W., Jamiru, T., & Chemere, E. B. (2025). Flame retardancy of biopolymers enhanced by bio-based flame retardants: A review. *Journal of Fire Sciences*, *43*(2), 79–114. https://doi.org/10.1177/07349041241309308
Nicolle, L., Casper, J., Willimann, M., Journot, C. M. A., Detampel, P., Einfalt, T., Grisch-Chan, H. M., Thöny, B., Gerber-Lemaire, S., & Huwyler, J. (2021). Development of Covalent Chitosan-Polyethylenimine Derivatives as Gene Delivery Vehicle: Synthesis, Characterization, and Evaluation. *International Journal of Molecular Sciences*, *22*(8), 3828. https://doi.org/10.3390/ijms22083828

Nikita, K., Nam, S. Y., & Vijayakumar, V. (2025). Chitosan-Based Membranes: A Comprehensive Review of Nanofiltration, Pervaporation, and Ion Exchange Applications. *Polysaccharides*, *6*(2), 31. https://doi.org/10.3390/polysaccharides6020031

Nuruzzaman, M., Mondal, M. I. H., Shathi, A. S., Rahman, M. A., Islam, M. J., Alam, M. S., Biswas, P. K., Yousuf, A., & Rana, M. S. (2025). Composite materials from waste plastics: A sustainable approach for waste management and resource utilization. *Polymers and Polymer Composites*, *33*. https://doi.org/10.1177/09673911251318542

Oladele, I. O., Okoro, C. J., Agbeboh, N. I., Betiku, O. T., & Adelani, S. O. (2024). Current application of recycled waste plastics as a sustainable material: A review on availability, processing and application. *Journal of Thermoplastic Composite Materials*, *38*(1), 277–301. https://doi.org/10.1177/08927057241248040

Onyishi, H. O., & Oluah, C. K. (2020). Effect of stretch ratio on the induced crystallinity and mechanical properties of biaxially stretched PET. *Phase Transitions*, *93*(9), 924–934. https://doi.org/10.1080/01411594.2020.1813291

Palanisamy, G., Muhammed, A. P., Thangarasu, S., & Oh, T. H. (2023). Investigating the Sulfonated Chitosan/Polyvinylidene Fluoride-Based Proton Exchange Membrane with fSiO2 as Filler in Microbial Fuel Cells. *Membranes*, *13*(9), 758. https://doi.org/10.3390/membranes13090758

Palumbo, O., Cimini, A., Trequattrini, F., Brubach, J.-B., Roy, P., & Paolone, A. (2021). Evidence of the CH···O HydrogenBonding in Imidazolium-Based Ionic Liquids from Far-Infrared Spectroscopy Measurements and DFT Calculations. *International Journal of Molecular Sciences*, *22*(11), 6155. https://doi.org/10.3390/ijms22116155

Patel, T., Lata, R., Arikibe, J. E., & Rohindra, D. (2025). Towards sustainable microplastic cleanup: Al/Fe ionotropic chitosan hydrogels for efficient PET removal. *Environmental Monitoring and Assessment*, *197*(3). https://doi.org/10.1007/s10661-025-13661-y

Paul, T., Nahid, F., Ifat-Al-Karim, M., & Haque, M. M. (2024). Structural and optical study of chitosan–graphene oxide composite through hydrothermal route. *AIP Advances*, *14*(11). https://doi.org/10.1063/5.0231060

Pintilie, S. C., Birsan, I. G., Tiron, L. G., Balta, S., & Ganea, D. (2017). Influence of ZnO Nanoparticle Size and Concentration on the Polysulfone Membrane Performance. *Materiale Plastice*, *54*(2), 257–261. https://doi.org/10.37358/mp.17.2.4828

Prasad, S. G., De, A., & De, U. (2011). Structural and Optical Investigations of Radiation Damage in Transparent PET Polymer Films. *International Journal of Spectroscopy*, *2011*(1), 1–7. https://doi.org/10.1155/2011/810936

Primc, G., & Mozetič, M. (2022). Hydrophobic Recovery of Plasma-Hydrophilized Polyethylene Terephthalate Polymers. *Polymers*, *14*(12), 2496. https://doi.org/10.3390/polym14122496
Radu, E.-R., Pandele, A. M., Tuncel, C., Miculescu, F., & Voicu, S. I. (2023). Preparation and Characterization of Chitosan/LDH Composite Membranes for Drug Delivery Application. *Membranes*, *13*(2), 179. https://doi.org/10.3390/membranes13020179

Roy, P. S., Garnier, G., Allais, F., & Saito, K. (2021). Strategic Approach Towards Plastic Waste Valorization: Challenges and Promising Chemical Upcycling Possibilities.

ChemSusChem, *14*(19), 4007–4027. https://doi.org/10.1002/cssc.202100904

Sahni, J. K., Chopra, S., Ahmad, F. J., & Khar, R. K. (2008). Potential prospects of chitosan derivative trimethyl chitosan chloride (TMC) as a polymeric absorption enhancer: synthesis, characterization and applications. *Journal of Pharmacy and Pharmacology*, *60*(9), 1111–1119. https://doi.org/10.1211/jpp.60.9.0001

Sahu, L. R., Jadhav, S. V., Ingole, P. G., Gogoi, A., Chatterjee, S., Borpatra Gohain, M., Goswami, S., Borah, D., Hazarika, G., Karki, S., Yadav, D., & Sawake, S. V. (2024). Polymeric Membranes for Liquid Separation: Innovations in Materials, Fabrication, and Industrial Applications. *Polymers*, *16*(23), 3240. https://doi.org/10.3390/polym16233240

Sari, M., Tamrin, T., Kaban, J., & Alfian, Z. (2021). A novel composite membrane pectin from Cyclea Barbata Miers blend with chitosan for accelerated wound healing. *Polymer Testing*, *99*, 107207. https://doi.org/10.1016/j.polymertesting.2021.107207

Schubert, S. W., Jensen, K., Clausen, K. S., Brask, J., Malmendal, A., Borch, K., Thomsen, T. B., Hunt, C. J., Westh, P., & Meyer, A. S. (2024). Relationships of crystallinity and reaction rates for enzymatic degradation of poly (ethylene terephthalate), PET. *ChemSusChem*, *17*(10). https://doi.org/10.1002/cssc.202301752

Shin, S.-K., Jeon, T.-W., Kim, Y.-J., Um, N., & Cho, N.-H. (2020). New Policy Framework with Plastic Waste Control Plan for Effective Plastic Waste Management. *Sustainability*, *12*(15), 6049. https://doi.org/10.3390/su12156049

Smith, B. (1999). Infrared spectral interpretation: a systematic approach. *Choice Reviews Online*, *36*(10), 36–5697. https://doi.org/10.5860/choice.36-5697

Solaja, O. M., Osifo, O. K., & Amoo, O. F. (2024). Empowering informal plastic recyclers: addressing socio-economic challenges and human rights awareness in Ogun State, Nigeria. *BMC Environmental Science*, *1*(1). https://doi.org/10.1186/s44329-024-00011-5

Stel'Makh, S. A., Beskopylny, N., Beskopylny, A. N., Meskhi, B., Mailyan, L. R., Dotsenko, N., Kotenko, M., & Shcherban', E. M. (2022). Nanomodified Concrete with Enhanced Characteristics Based on River Snail Shell Powder. *Applied Sciences*, *12*(15), 7839. https://doi.org/10.3390/app12157839

Su, C., Berekute, A. K., & Yu, K.-P. (2022). Chitosan@TiO2 composites for the adsorption of copper(II) and antibacterial applications. *Sustainable Environment Research*, *32*(1). https://doi.org/10.1186/s42834-022-00138-7

Sui, Y., Luo, S., Qu, L., Li, P., Zhang, C., Dai, X., & Zhang, J. (2020). A green self-assembled organic supermolecule as an effective flame retardant for epoxy resin. *RSC Advances*, *10*(21), 12492–12503. https://doi.org/10.1039/d0ra00072h

Sun, X., Yin, L., Zhu, H., Zhu, J., Hu, J., Luo, X., Huang, H., & Fu, Y. (2022). Enhanced Antimicrobial Cellulose/Chitosan/ZnO Biodegradable Composite Membrane. *Membranes*, *12*(2), 239. https://doi.org/10.3390/membranes12020239

Suneetha, R. B. (2018). Spectral, Thermal and Morphological Characterization of Biodegradable Graphene Oxide-Chitosan Nanocomposites. *Journal of Nanoscience and Technology*, *04*(02), 342–344. https://doi.org/10.30799/jnst.sp208.18040201

Szopa, D., Pstrowska, K., & Witek-Krowiak, A. (2025). Chitosan-Coated Alginate Matrices with Protein-Based Biostimulants: A Controlled-Release System for Sustainable Agriculture. *Materials (Basel, Switzerland)*, *18*(3), 591. https://doi.org/10.3390/ma18030591

Tamburaci, S., & Tihminlioglu, F. (2017). Novel poss reinforced chitosan composite membranes for guided bone tissue regeneration. *Journal of Materials Science: Materials in Medicine*, *29*(1). https://doi.org/10.1007/s10856-017-6005-5

Thanh, N. T., Kumar, P., Duy, D. V., Toan, P. V., Minh, H. V. T., Tantray, F. A., Ty, T. V., Meraj, G., & Lavane, K. (2024). Assessment and Sustainable Management Strategies for Plastic Waste in Can Tho City, Vietnam: A Circular Economy Approach. *Water*, *16*(7), 951. https://doi.org/10.3390/w16070951

Then, J., Wei, R., Oeser, T., Gerdts, A., Schmidt, J., Barth, M., & Zimmermann, W. (2016). A disulfide bridge in the calcium binding site of a polyester hydrolase increases its thermal stability and activity against polyethylene terephthalate. *FEBS Open Bio*, *6*(5), 425–432. https://doi.org/10.1002/2211-5463.12053

Thomsen, T. B., Almdal, K., & Meyer, A. S. (2023). Significance of poly(ethylene terephthalate) (PET) substrate crystallinity on enzymatic degradation. *New Biotechnology*, *78*, 162–172. https://doi.org/10.1016/j.nbt.2023.11.001

Uchechukwu Nwafor, G. (2024). Impact of Plastic Pollution on the Economic Growth and Sustainability of Blue Economy in Nigeria. *African Journal of Environment and Natural Science Research*, *7*(1), 113–127. https://doi.org/10.52589/ajensr-hhv6sbjf

Unfried, K., & Wang, F. (2024). Importing air pollution? Evidence from China's plastic waste imports. *Journal of Environmental Economics and Management*, *125*, 102996. https://doi.org/10.1016/j.jeem.2024.102996

Vafakish, B., & Wilson, L. D. (2019). Surface-Modified Chitosan: An Adsorption Study of a "Tweezer-Like" Biopolymer with Fluorescein. *Surfaces*, *2*(3), 468–484. https://doi.org/10.3390/surfaces2030035

Vasilev, A., Dzidziguri, E., Efimov, M., Bondarenko, G., Kozlov, V., & Karpacheva, G. (2019). Thermal behavior of chitosan as a carbon material precursor under IR radiation.

ISSN: **3107-6513**

IOP Conference Series: Materials Science and Engineering, *693*(1), 012002. https://doi.org/10.1088/1757-899x/693/1/012002

Villanueva, C. M., Garfí, M., Milà, C., Olmos, S., Ferrer, I., & Tonne, C. (2021). Health and environmental impacts of drinking water choices in Barcelona, Spain: A modelling study. *Science of The Total Environment*, *795*, 148884. https://doi.org/10.1016/j.scitotenv.2021.148884

Xing, K., Zhu, X., Peng, X., & Qin, S. (2014). Chitosan antimicrobial and eliciting properties for pest control in agriculture: a review. *Agronomy for Sustainable Development*, *35*(2), 569–588. https://doi.org/10.1007/s13593-014-0252-3

Xu, B., Ma, W., Qian, L., Shao, L., & Bi, X. (2019). Synergistic Effects of Nano-zinc Oxide on Improving the Flame Retardancy of EVA Composites with an Efficient Triazine-Based Charring Agent. *Journal of Polymers and the Environment*, *27*(5), 1127–1140. https://doi.org/10.1007/s10924-019-01400-7

Yang, X. J., Zhong, J. X., Li, A., & Glaser, R. (2016). The C–H Stretching features at 3.2–3.5 μm of Polycyclic Aromatic Hydrocarbons with Aliphatic Sidegroups. *The Astrophysical Journal*, *825*(1), 22. https://doi.org/10.3847/0004-637x/825/1/22

Zakaria, Z., Izzah, Z., Hassan, A., & Jawaid, M. (2012). Effect of Degree of Deacetylation of Chitosan on Thermal Stability and Compatibility of Chitosan-Polyamide Blend. *BioResources*, *7*(4). https://doi.org/10.15376/biores.7.4.5568-5580

Zhu, B., Yoshie, N., He, Y., Li, J., & Inoue, Y. (2003). Hydrogen-Bonding Interaction and Crystalline Morphology in the Binary Blends of Poly(ε-caprolactone) and Polyphenol Catechin. *Macromolecular Bioscience*, *3*(11), 684–693. https://doi.org/10.1002/mabi.200350034